

# Infrared Evidence of a Formate-Intermediate Mechanism over Ca-Modified Supports in Low-Temperature Ethanol Steam Reforming

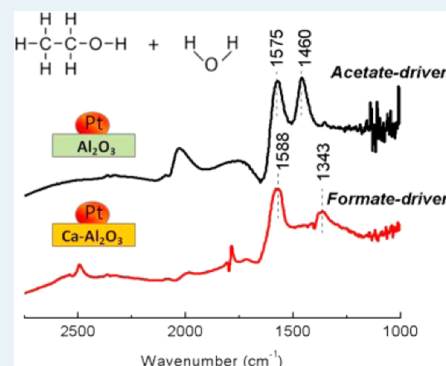
Catherine Choong,<sup>†,‡</sup> Ziyi Zhong,<sup>†</sup> Lin Huang,<sup>†</sup> Armando Borgna,<sup>†</sup> Liang Hong,<sup>\*,‡</sup> Luwei Chen,<sup>\*,†</sup> and Jianyi Lin<sup>†</sup>

<sup>†</sup>Institute of Chemical and Engineering Sciences, A\*STAR (Agency for Science, Technology and Research), 1 Pesek Road, Jurong Island, Singapore 627833

<sup>‡</sup>Department of Chemical and Biomolecular Engineering, National University of Singapore, 10 Kent Ridge Crescent, Singapore 119260

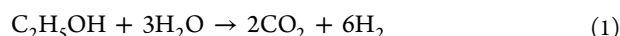
## S Supporting Information

**ABSTRACT:** An *in situ* DRIFTS study of ethanol adsorption and desorption was performed on Pt (Rh, Pd) supported on Al<sub>2</sub>O<sub>3</sub> and Ca-Al<sub>2</sub>O<sub>3</sub>. Different from the well-known acetate-intermediate reaction mechanism observed on Al<sub>2</sub>O<sub>3</sub>-supported metal catalysts, formate species are exclusively observed on Pt (Rh, Pd) supported on Ca-Al<sub>2</sub>O<sub>3</sub>, offering a new mechanism denoted as the formate-intermediate mechanism. The key factor in determining the change in mechanism is the reduced availability of surface oxygen and the enhanced C–C breaking ability of the metal catalyst upon Ca modification. The formate-intermediate mechanism is favored in the presence of noble metals in the following order: Pt > Rh > Pd.

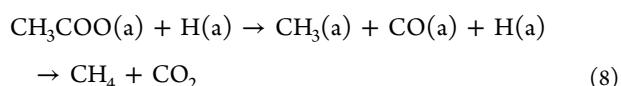
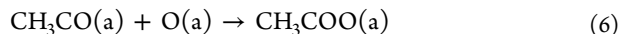
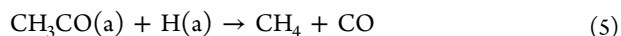
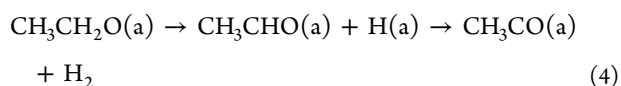
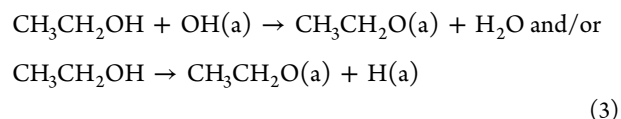
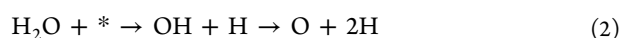


**KEYWORDS:** ethanol steam reforming, reaction pathway, acetate, formate, Pt, Rh, Pd, Ca, Al<sub>2</sub>O<sub>3</sub>

Catalytic ethanol steam reforming (ESR, eq 1) is a promising reaction for renewable hydrogen production and has been extensively explored over the past decade.<sup>1</sup>



However, the complexity of the reaction network and the large number of intermediates presented during the reaction pose challenges in elucidating the reaction pathways.<sup>2</sup> A number of ESR mechanistic studies using Fourier transform infrared spectroscopy (FTIR) over supported noble metal catalysts have been conducted.<sup>3–7</sup> One generally proposed mechanism involves the participation of acetates via dehydrogenation and subsequent oxidation from ethoxides (eqs 2–8). Surface-adsorbed water dissociates into surface hydroxyls and/or lattice oxygen (eq 2). Ethoxides and acetates were detected at different temperatures upon ethanol adsorption (eq 3). Ethoxides can either decompose into H<sub>2</sub>, CO, and CH<sub>4</sub> or undergo dehydrogenation (eq 4), producing acetaldehyde and acetyl, which may further decompose to CO and CH<sub>4</sub> (eq 5). The reaction of acetaldehyde and acetyl groups with lattice oxygen (eq 6) or surface hydroxyls (eq 7) leads to formation of the acetate intermediate and the final products (eq 8).<sup>3</sup> Herein, we denote the reaction pathway shown below as the acetate-intermediate pathway.



Recently, the coexistence of formate and acetate species on Al<sub>2</sub>O<sub>3</sub>-supported Pt catalysts was reported by both Panagioutopoulou et al. and Sanchez-Sanchez et al.<sup>7,8</sup> Very weak IR bands of formate species were also reported over unreduced Pt/CeO<sub>2</sub> by Yee et al.<sup>9</sup> In our previous study of the Fe-promoted Rh/Ca-Al<sub>2</sub>O<sub>3</sub> catalyst, formate species were proposed as an important

Received: March 18, 2014

Revised: June 11, 2014

Published: June 12, 2014

intermediate in ESR.<sup>10</sup> Therefore, an alternative to the acetate-intermediate pathway may exist over these catalysts, which we would denote as the formate-intermediate mechanism. The Ca-modified  $\text{Al}_2\text{O}_3$  support has proven to be beneficial in ethanol steam reforming because of the modification of the acidic versus basic properties of  $\text{Al}_2\text{O}_3$ , resulting in an increase in the surface density of active metals by weakening the metal–support interaction.<sup>11,12</sup> In addition, the presence of Ca reduces the extent of coke formation by reducing the metal particle size and generating more surface hydroxyls.<sup>11,12</sup> In this letter, to elucidate the role of catalyst support and metal in the determination of ESR pathways, we report an *in situ* DRIFTS study of ethanol adsorption and temperature-programmed desorption (TPD) on three noble metals catalysts (Pt, Rh, and Pd, each at 1 wt % loading) supported on  $\text{Ca-Al}_2\text{O}_3$  and  $\text{Al}_2\text{O}_3$ , respectively. A formate-intermediate pathway was first proposed.

The synthesis of catalysts is described in detail in the Supporting Information. Spectroscopic experiments were performed using a Bio-Rad FT-IT 3000 MX instrument equipped with a high-temperature cell fitted with KBr windows and a mercury–cadmium–telluride (MCT-A) detector. The sample was reduced in  $\text{H}_2$  ( $20 \text{ mL min}^{-1}$ ) at 473 K for 2 h and cooled in He ( $20 \text{ mL min}^{-1}$ ) to 303 K. Subsequently, ethanol was introduced into the cell with a He flow ( $50 \text{ mL min}^{-1}$ ) through a saturator for 20 min. Following this, the sample was flushed with He ( $50 \text{ mL min}^{-1}$ ) to remove physically adsorbed ethanol. The sample was heated to different temperatures in He ( $50 \text{ mL min}^{-1}$ ). Spectra were recorded at 303–673 K at a resolution of  $4 \text{ cm}^{-1}$  with typically more than 256 scans. The freshly reduced sample was used as a reference.

Figure 1a shows spectra for the adsorption of ethanol on Pt/ $\text{Al}_2\text{O}_3$  during progressive heating. At 303 K, molecularly adsorbed ethanol and dissociative intermediates are observed. The bands at  $1386 \text{ cm}^{-1}$  [ $\delta(\text{CH}_3)$  in ethanol] and  $1277 \text{ cm}^{-1}$  [ $\delta(\text{OH})$  in ethanol] correspond to molecularly adsorbed ethanol, which may bond to surface OH groups via H-bonding and/or Lewis acid sites ( $\text{Al}^{3+}$ ) on the oxidic support.<sup>13</sup> Negative bands located at  $3742$  and  $3700 \text{ cm}^{-1}$  reveal the loss of surface OH groups over the  $\text{Al}_2\text{O}_3$  support, which may interact with the molecularly adsorbed ethanol as indicated in eq 3. The presence of C–H stretching bands at  $2971 \text{ cm}^{-1}$  [ $\nu_a(\text{CH}_3)$ ],  $2935 \text{ cm}^{-1}$  [ $\nu_a(\text{CH}_2)$ ], and  $2880 \text{ cm}^{-1}$  [ $\nu_s(\text{CH}_3)$ ] and C–C–O stretching of ethoxy species at  $1164 \text{ cm}^{-1}$  indicates ethoxide species are formed via the dissociative adsorption of ethanol. Further decomposition and oxidation of adsorbed ethoxide lead to the detection of a strongly adsorbed CO band (eq 5) at  $2036 \text{ cm}^{-1}$ . The predominant bands at  $1575$  and  $1460 \text{ cm}^{-1}$  with an intensity ratio of 1:1 can be assigned to asymmetric and symmetric O–C–O stretching, respectively,<sup>3</sup> because of the presence of acetate, resulting from the dehydrogenation of ethoxide and the subsequent oxidation by lattice O or OH groups (eqs 6 and 7). In addition, three shoulders can be observed in the lower-frequency region. The peak at  $1340 \text{ cm}^{-1}$  between 303 and 473 K may be assigned to formate species.<sup>14–16</sup> The signals of molecularly adsorbed ethanol remain observable until 473 K but disappear at 523 K, an observation consistent with our ethanol adsorption and TPD (Figure S1 of the Supporting Information) and the literature.<sup>3</sup> Similarly, the intensities of bands of the ethoxide species decrease with an increase in temperature and become scarcely detectable at 523 K. On the other hand, the intensities of the CO and acetate bands increase as the temperature increases (up

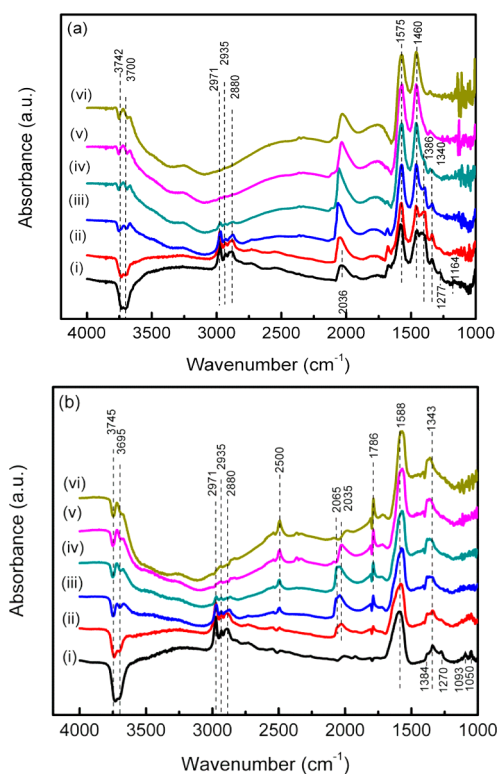


**Figure 1.** DRIFTS spectra at various temperatures after  $\text{C}_2\text{H}_5\text{OH}$  adsorption on (a) Pt/ $\text{Al}_2\text{O}_3$  and (b) Pt/ $\text{Ca-Al}_2\text{O}_3$ . The spectra were recorded at (i) 303 K after ethanol adsorption followed by He purge and (ii–vi) 373, 473, 523, 573, and 673 K, respectively.

to 673 K), progressively. The negative bands, which are associated with hydrogen-bonded hydroxyls, in the region between  $3200$  and  $3600 \text{ cm}^{-1}$  become less intense as the temperature increases from 473 to 673 K. This suggests the dissociation and consumption of surface hydroxyl groups as the temperature increases. The DRIFTS results of Pt/ $\text{Al}_2\text{O}_3$  described above are in good agreement with the literature on Pt/ $\text{Al}_2\text{O}_3$ , suggesting the acetate-intermediate mechanism.<sup>17</sup>

The spectra of adsorbed ethanol over Pt/ $\text{Ca-Al}_2\text{O}_3$  are shown in Figure 1b. At 303 K, the appearance of adsorbed ethanol, ethoxides, and the negative OH bands on Pt/ $\text{Ca-Al}_2\text{O}_3$  is similar to the appearance of those on Pt/ $\text{Al}_2\text{O}_3$ . However, there are two significant differences for Pt/ $\text{Ca-Al}_2\text{O}_3$ . First, the characteristic acetate band at  $1460 \text{ cm}^{-1}$  is not observed. Instead, two predominant bands appear at  $1588$  and  $1340 \text{ cm}^{-1}$ . These two bands shift to  $1575$  and  $1360 \text{ cm}^{-1}$ , respectively, when the temperature gradually increases from 303 to 673 K. The maximal intensity is observed at 673 K. To identify the peaks, acetic acid, formic acid, and carbon dioxide were individually adsorbed over reduced Pt/ $\text{Ca-Al}_2\text{O}_3$  (see Figure S2 of the Supporting Information). Clearly, the peaks at  $1575$ – $1588$  and  $1340$ – $1360 \text{ cm}^{-1}$  coincide with the asymmetric and symmetric O–C–O stretching vibrations, respectively, of formate species adsorbed on the catalyst (Figure S2d of the Supporting Information).<sup>16</sup> In addition, the symmetric band of the O–C–O stretch at  $1575 \text{ cm}^{-1}$ , which has one-third of the intensity of its asymmetric band at  $1360 \text{ cm}^{-1}$ , further affirms the presence of formate species at higher temperatures.<sup>18</sup> This is the first time that formate species have been clearly identified.

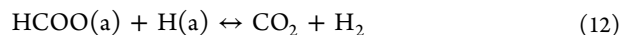
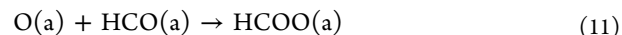
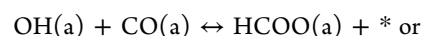
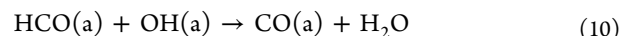
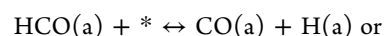
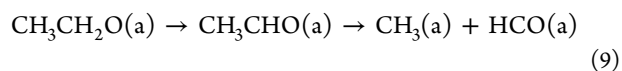
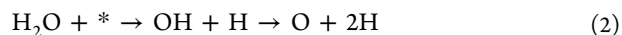
The second noticeable difference between Pt/ $\text{Al}_2\text{O}_3$  and Pt/ $\text{Ca-Al}_2\text{O}_3$  is that the CO band is not evident on Pt/ $\text{Ca-Al}_2\text{O}_3$  at

303 K. CO adsorption is associated with the dissociation of ethoxide species. The smaller amount of adsorbed CO on Pt/Ca-Al<sub>2</sub>O<sub>3</sub> at 303 K suggests that ethoxide species are more stable on Pt/Ca-Al<sub>2</sub>O<sub>3</sub> than on Pt/Al<sub>2</sub>O<sub>3</sub>. This is because the Ca-modified catalysts have a higher affinity for water adsorption and the adsorbed water is found to be able to stabilize the ethoxide species at room temperature.<sup>19</sup> Progressive heating of the sample leads to the loss of molecularly adsorbed ethanol as well as ethoxide species. This is seen in the decreasing intensity of the corresponding bands at 1384, 1270, 1095, 1054, 2971, 2935, and 2880 cm<sup>-1</sup> (Figure 1b). It is observed that the loss of ethoxide runs parallel to the increase in CO adsorption on Pt/Ca-Al<sub>2</sub>O<sub>3</sub> between 373 and 523 K. Between 373 and 523 K, two vibration modes of linearly adsorbed CO are observed: CO adsorbed on partially oxidized Pt<sup>δ+</sup> [ $\nu(\text{CO}) = 2065 \text{ cm}^{-1}$ ] and CO adsorbed on reduced Pt<sup>0</sup> particles [ $\nu(\text{CO}) = 2035 \text{ cm}^{-1}$ ].<sup>7</sup> The presence of partially oxidized Pt<sup>δ+</sup> could be due to the oxidation of Pt<sup>0</sup> by surface oxygen deriving from dissociation of CO or H<sub>2</sub>O. The intensity of  $\nu(\text{CO})$  bands starts to decrease at  $\geq 573 \text{ K}$ , leaving a weak band at 2000 cm<sup>-1</sup>. Similar to the data in Figure 1a, the intensity of the bands in the region between 3200 and 3600 cm<sup>-1</sup> decreases at 473–673 K, indicating the dissociation and consumption of surface hydroxyls as the temperature increases. At 473 K, two new bands at 2500 and 1786 cm<sup>-1</sup> are observed. These two bands are not observed in Figure 1a, which indicates that these bands are associated with the presence of Ca species. Several authors have assigned the peak at 1786 cm<sup>-1</sup> to the  $\nu(\text{CO})$  mode of adsorbed acetaldehyde.<sup>19,20</sup> However, it is shown through ethanol adsorption and TPD in Figure S1a of the Supporting Information that acetaldehyde decomposes completely at approximately 550 K. Therefore, the peak at 1786 cm<sup>-1</sup> is unlikely to be related to adsorbed acetaldehyde because the marked increase in its intensity occurs between 473 and 673 K. Instead, it is more reasonable to assign the two peaks to the H–OC and HC=O stretches of adsorbed HCO species, respectively.<sup>21,22</sup> The formation of these species will require the cleavage of the C–C bond with the assistance of active metal sites, and it cannot occur over the Ca-Al<sub>2</sub>O<sub>3</sub> support alone, especially at low temperatures.

Early surface science study of the adsorption of ethanol on Ni(111) and Pt surfaces revealed that the adsorption of ethanol on Ni(111) or Pt surfaces is dissociative following the (i) O–H, (ii) C<sub>α</sub>–H, (iii) C–C, (iv) C<sub>β</sub>–H bond scission sequence.<sup>23,24</sup> Recent density functional theory (DFT) calculation of ESR on Pt indicated that the activation energy for C–C scission decreases with increasing levels of ethanol dehydrogenation.<sup>25</sup> C–H bond scission leads to a coordinatively unsaturated ketyl or acetyl carbon atom, which may then be stabilized by forming metal–carbon bonds, causing a weakening of the C–C bond. The DFT calculation also showed that oxidative dehydrogenation by surface OH groups is energetically more favorable than thermal decomposition of ethanol without the assistance of surface OH groups. The oxidative dehydrogenation is not remarkable on Ca-free Pt/Al<sub>2</sub>O<sub>3</sub> catalysts because of the low coverage of adsorbed OH. However, oxidative dehydrogenation (e.g., C<sub>β</sub>–H) and thus C–C cracking are expected on the Ca-promoted Pt/Al<sub>2</sub>O<sub>3</sub> catalyst because of the presence of abundant OH groups. Therefore, C–C bond scission may occur on Ca-Al<sub>2</sub>O<sub>3</sub>-supported Pt catalysts, leading to the generation of adsorbed HCO (eq 9). The C=O carbonyl vibration is typically observed at 1786 cm<sup>-1</sup> in Figure 1b, while the H–C stretching vibration is shifted

to 2500 cm<sup>-1</sup>. This is understandable if the hydrogen atom of HCO is bonded to adsorbed oxygen on Ca-Al<sub>2</sub>O<sub>3</sub>, forming a CaO...H...C=O species. The downshift of the C–H vibration (to 2715 cm<sup>-1</sup>) caused by H-bonding was previously reported by Iwasawa et al. for the bidentate formate.<sup>15</sup> In the presence of abundant surface OH groups, the adsorbed CO or HCO species on the catalyst surface can be converted to formate species HCOO (eqs 10–11). The HCOO intermediate may undergo either dehydration (to CO) or dehydrogenation (to H<sub>2</sub> and CO<sub>2</sub>) (eq 12), depending on the structure of the formate. Previous studies showed that bidentate formate favors dehydrogenation while monodentate leads to dehydration.<sup>14,15</sup> Surface-adsorbed water was reported to assist 100% dehydrogenation of formate on oxide-supported Rh catalysts.<sup>15</sup> Obviously, the formate species on Pt/Ca-Al<sub>2</sub>O<sub>3</sub> with characteristic COO vibrations at 1575 and 1360 cm<sup>-1</sup> (Figure 1b and Figure S2e of the Supporting Information) are bidentate, and the presence of adsorbed water (or surface OH groups) can further enhance dehydrogenation of the formate intermediates, producing CO<sub>2</sub> and H<sub>2</sub> upon heating (eq 12).

At present, spectroscopic evidence clearly shows that the modification of alumina by calcium has altered the reaction pathway of ESR from the one mediated by acetates (acetate-intermediate) over Pt/Al<sub>2</sub>O<sub>3</sub> to the one aided by formate species (formate-intermediate) over Pt/Ca-Al<sub>2</sub>O<sub>3</sub>. Therefore, our results unravel a new mechanism for ethanol reforming over Ca-Al<sub>2</sub>O<sub>3</sub>-supported Pt catalysts, the formate-intermediate reaction pathway:



The formate-intermediate pathway is also observed over Rh and Pd catalysts. On Rh/Ca-Al<sub>2</sub>O<sub>3</sub> (Figure 2a), adsorption bands [ $\nu_{\text{a}}(\text{O}-\text{C}-\text{O}) = 1572 \text{ cm}^{-1}$ , and  $\nu_{\text{s}}(\text{O}-\text{C}-\text{O}) = 1380 \text{ cm}^{-1}$ ] at 473 K are attributed to formate species, and the intensities of these bands gradually increase as the temperature increases. The two bands at 2030 and 1830 cm<sup>-1</sup> correspond to linear and bridge-bonded Rh-CO, respectively. At high temperatures (>573 K), the depletion of hydroxyl and the appearance of HCO species (H–OC and HC=O stretches at 2495 and 1784 cm<sup>-1</sup>, respectively) are similarly observed in Figure 1b. On Pd/Ca-Al<sub>2</sub>O<sub>3</sub> (Figure 2b), the presence of formate species is evidenced by an intense band at 1609 cm<sup>-1</sup> along with a band located at 1339 cm<sup>-1</sup>.<sup>26</sup> However, the IR band at 1930 cm<sup>-1</sup>, which can be attributed to bridge-bonded CO, is rather weak on Pd.<sup>27</sup> TPD of ethanol over Pd/Ca-Al<sub>2</sub>O<sub>3</sub> indicates the desorption of CO and H<sub>2</sub> at 657 K, whereas CO is essentially converted to CO<sub>2</sub> over Pt and Rh catalysts (Figure S1 of the Supporting Information). DFT calculations showed that the ability of Pd to adsorb CO is not as good as those of other noble metals such as Pt, Rh, Ru, Os, and Ir, which could probably explain why Pd is less active for the catalytic ESR

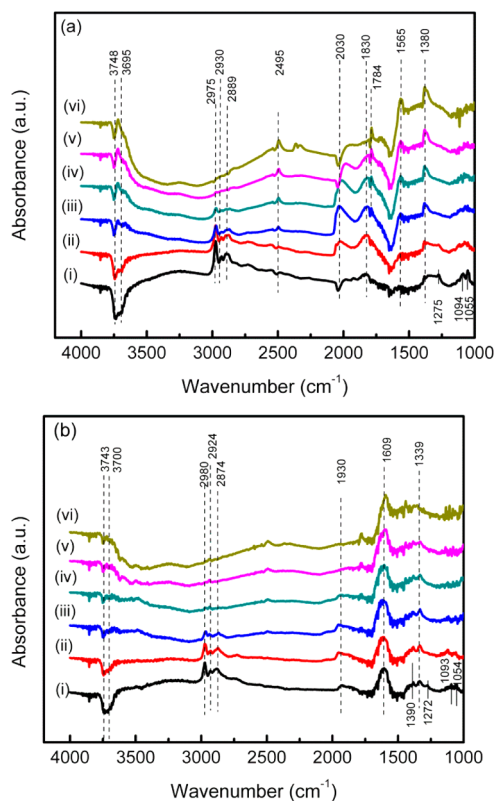


**Figure 2.** DRIFTS spectra at various temperatures after  $C_2H_5OH$  adsorption on (a) Rh/Ca- $Al_2O_3$  and (b) Pd/Ca- $Al_2O_3$ . The spectra were recorded at (i) 303 K after ethanol adsorption followed by He purge and (ii–vi) 373, 473, 523, 573, and 673 K, respectively.

reaction in this contribution (Table S1 of the Supporting Information).<sup>28</sup> Here, the reaction mechanism over Rh/Ca- $Al_2O_3$  and Pd/Ca- $Al_2O_3$  is similar to that of Pt/Ca- $Al_2O_3$ , i.e., formate-intermediate pathway. The weak IR bands belonging to formate species and adsorbed CO suggest poorer WGS activity on Rh and Pd than on Pt catalysts, an observation that is in agreement with the literature.<sup>29</sup>

As indicated above, over the Ca- $Al_2O_3$ -supported Pt, Rh, and Pd catalysts, ESR follows the formate-intermediate pathway, which suggests that formate formation is independent of the nature of the active metal. This is consistent with the conclusion of Erdöhelyi et al., who observed the formation of surface acetates over  $Al_2O_3$ -supported Rh, Ir, Ru, Pd, and Pt catalysts.<sup>3</sup> Therefore, the change from the acetate- to formate-intermediate reaction pathway in this study is solely related to the changes in the surface properties of the support induced by Ca addition.

Formation of acetates from ethanol adsorption has been widely reported over various oxides, such as  $Al_2O_3$ , MgO, and  $CeO_2$ .<sup>6,30–32</sup> A structural change from an ethoxide to an acetate species occurs via dehydrogenation to form an acyl group that is subsequently oxidized to form acetate. Yee et al. studied ethanol adsorption over unreduced  $CeO_2$ , reduced  $CeO_2$ , and Pd/ $CeO_2$ .<sup>6</sup> Their results show that surface oxygen atoms on unreduced  $CeO_2$  are responsible for acetate formation. On the other hand, the formation of acetate is not observed on the reduced  $CeO_2$  because of the depletion of surface oxygen atoms. The presence of Pd facilitates partial reduction of  $CeO_2$ , which also leads to no acetate formation over reduced Pd/ $CeO_2$ . Therefore, the high availability of oxygen atoms on the

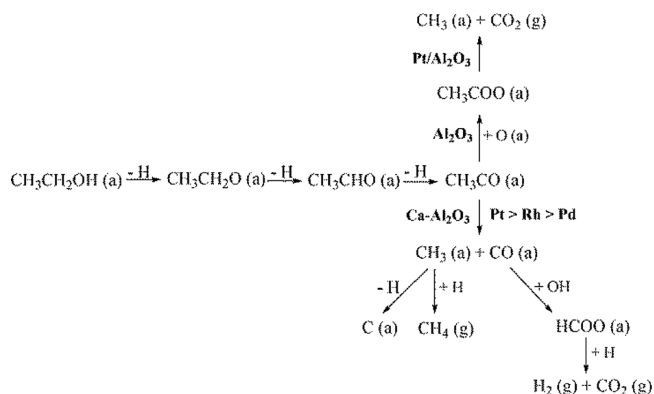
support favors the oxidation of carboxyl carbon to acetate.<sup>30</sup> Similar to the results reported by Yee et al., on the surfaces of Ca-free  $Al_2O_3$  and Pt/ $Al_2O_3$  catalysts, there are large numbers of surface oxide ions in close interaction with the adsorbed ethoxide/acetaldehyde (located at  $Al^{3+}$  Lewis acidic centers or Pt sites at the metal–oxide interface), favoring the formation of acetate species as evidenced in Figure 1a and the literature.<sup>3,6,31,33</sup>

The presence of Ca induced significant changes in the surface properties, thereby altering the reaction pathway.<sup>11,12</sup> Our previous DRIFTS studies clearly showed that ethoxide was not formed at 673 K while acetates were observed over  $Al_2O_3$ . In contrast, ethoxide species were detected over Ca- $Al_2O_3$  at 673 K, without observable bands attributed to either acetate or formate species. Characterization of the Ca- $Al_2O_3$  surface showed a large amount of adsorbed water on the surface of the sample.<sup>11</sup> These species and the presence of Ca might block surface oxygen sites that closely interact with the active sites, hindering the formation of acetate species.<sup>33</sup> In addition, on the basis of DFT calculations, the presence of extra OH groups can facilitate the formation of  $CO_2$  through COO–H bond breaking, which has almost no energy barrier.<sup>34</sup>

It is worth noting that the formate species can be observed only in the presence of an active metal on Ca- $Al_2O_3$ . Previous studies of a Ni catalyst supported on Ca-modified  $Al_2O_3$  have shown that Ca modification on  $Al_2O_3$  prevents the formation of nickel aluminates, resulting in higher Ni concentrations on the surface of the catalyst. In addition, an electron density near the Fermi level due to the contribution of Ni 3d is enhanced due to the presence of Ca.<sup>12</sup> Similarly, on the Pt/Ca- $Al_2O_3$  catalyst, Ca can increase the electronic density of the catalyst. This electronic modification on Pt will enhance the adsorption of the alcohol on the catalyst, causing an increase in the stability of the ethoxides as shown by DRIFTS.<sup>32</sup> On the other hand, the presence of abundant surface OH groups can facilitate the dehydrogenation of adsorbed ethanol, reducing the activation energy of C–C bond cracking. Hence, ethanol adsorption and reaction on Ca- $Al_2O_3$ -supported Pt catalysts may follow the new formate-intermediate reaction pathway shown in Scheme 1. HCO is first formed and reacts with adjacent OH or O, generating formate species (HCOO) on the surface (eq 11). The HCOO intermediates further undergo dehydrogenation to generate  $H_2$  and  $CO_2$  (eq 12).

In conclusion, the reaction pathways of ESR on noble metals (Pt, Rh, and Pd) supported on  $Al_2O_3$  and Ca- $Al_2O_3$  were

### Scheme 1. Reaction Pathways of Ethanol over $Al_2O_3$ - and Ca- $Al_2O_3$ -Supported Noble Metals



thoroughly investigated using *in situ* DRIFTS, ethanol TPD, and steady-state catalytic testing. The ESR pathway over Pt/Al<sub>2</sub>O<sub>3</sub> involves the formation of acetates. In contrast, the presence of Ca in the Pt/Ca-Al<sub>2</sub>O<sub>3</sub> catalyst alters the reaction pathway from the acetate- to formate-intermediate pathway. This is due to the deficiency of surface oxygen as well as an increase in the Fermi level upon Ca modification. The proposed reaction pathways are illustrated in Scheme 1. This is the first time that the formate-intermediate reaction pathway for ESR is clearly revealed by an *in situ* FTIR study.

## ■ ASSOCIATED CONTENT

### ● Supporting Information

Experimental details; DRIFTS spectra of ethanol, acetic acid, formic acid, and CO<sub>2</sub>; catalytic activity; and temperature-programmed desorption of ethanol. This material is available free of charge via the Internet at <http://pubs.acs.org>.

## ■ AUTHOR INFORMATION

### Corresponding Authors

\*E-mail: [chen\\_luwe@ices.a-star.edu.sg](mailto:chen_luwe@ices.a-star.edu.sg).

\*E-mail: [chehongl@ices.a-star.edu.sg](mailto:chehongl@ices.a-star.edu.sg).

### Notes

The authors declare no competing financial interest.

## ■ ACKNOWLEDGMENTS

We gratefully acknowledge the financial support from the Agency of Science, Technology and Research (A\*STAR), Singapore.

## ■ REFERENCES

- (1) Yamazaki, T.; Kikuchi, N.; Katoh, M.; Hirose, T.; Saito, H.; Yoshikawa, T.; Wada, M. *Appl. Catal., B* **2010**, *99*, 81–88.
- (2) Mattos, L. V.; Jacobs, G.; Davis, B. H.; Noronha, F. B. *Chem. Rev.* **2012**, *112*, 4094–4123.
- (3) Erdöhelyi, A.; Raskó, J.; Kecskés, T.; Tóth, M.; Dömök, M.; Baán, K. *Catal. Today* **2006**, *116*, 367–376.
- (4) Jacobs, G.; Keogh, R. A.; Davis, B. H. *J. Catal.* **2007**, *245*, 326–337.
- (5) Song, H.; Bao, X.; Hadad, C.; Ozkan, U. *Catal. Lett.* **2011**, *141*, 43–54.
- (6) Yee, A.; Morrison, S. J.; Idriss, H. *J. Catal.* **1999**, *186*, 279–295.
- (7) Panagiotopoulou, P.; Verykios, X. E. *Int. J. Hydrogen Energy* **2012**, *37*, 16333–16345.
- (8) Sanchez-Sanchez, M. C.; Navarro Yerga, R. M.; Kondarides, D. I.; Verykios, X. E.; Fierro, J. L. G. *J. Phys. Chem. A* **2010**, *114*, 3873–3882.
- (9) Yee, A.; Morrison, S. J.; Idriss, H. *J. Catal.* **2000**, *191*, 30–45.
- (10) Chen, L.; Choong, C.; Zhong, Z.; Huang, L.; Ang, T. P.; Hong, L.; Lin, J. *J. Catal.* **2010**, *276*, 197–200.
- (11) Choong, C.; Huang, L.; Zhong, Z.; Lin, J.; Hong, L.; Chen, L. *Appl. Catal., A* **2011**, *407*, 155–162.
- (12) Choong, C.; Zhong, Z.; Huang, L.; Wang, Z.; Ang, T. P.; Borgna, A.; Lin, J.; Hong, L.; Chen, L. *Appl. Catal., A* **2011**, *407*, 145–154.
- (13) Raskó, J.; Dömök, M.; Baán, K.; Erdöhelyi, A. *Appl. Catal., A* **2006**, *299*, 202–211.
- (14) Lin, J.; Neoh, K. G.; Teo, W. K. *J. Chem. Soc., Faraday Trans.* **1994**, *9*, 355–362.
- (15) Shido, T.; Asakura, K.; Iwasawa, Y. *J. Catal.* **1990**, *122*, 55–56.
- (16) Solymosi, F.; Koós, Á.; Liliom, N.; Ugrai, I. *J. Catal.* **2011**, *279*, 213–219.
- (17) Dömök, M.; Tóth, M.; Raskó, J.; Erdöhelyi, A. *Appl. Catal., B* **2007**, *69*, 262–272.
- (18) Hertl, W.; Cuenca, A. M. *J. Phys. Chem.* **1973**, *77*, 1120–1126.
- (19) Idriss, H.; Diagne, C.; Hindermann, J. P.; Kiennemann, A.; Barteau, M. A. *J. Catal.* **1995**, *155*, 219–237.
- (20) Silva, A. M.; Costa, L. O. O.; Barandas, A. P. M. G.; Borges, L. E. P.; Mattos, L. V.; Noronha, F. B. *Catal. Today* **2008**, *133–135*, 755–761.
- (21) Raskó, J.; Kiss, J. *Appl. Catal., A* **2005**, *287*, 252–260.
- (22) Cabilla, G. C.; Bonivardi, A. L.; Baltanás, M. A. *Appl. Catal., A* **2003**, *255*, 181–195.
- (23) Gates, S. M.; Russell, J. N., Jr.; Yates, J. T., Jr. *Surf. Sci.* **1986**, *171*, 111–134.
- (24) Mavrikakis, M.; Barteau, M. A. *J. Mol. Catal. A: Chem.* **1998**, *131*, 135–147.
- (25) Sutton, J. E.; Panagiotopoulou, P.; Verykios, X. E.; Vlachos, D. G. *J. Phys. Chem. C* **2013**, *117*, 4691–4706.
- (26) Borchert, H.; Jürgens, B.; Zielasek, V.; Rupprechter, G.; Giorgio, S.; Henry, C. R.; Bäumer, M. *J. Catal.* **2007**, *247*, 145–154.
- (27) Maroto-Valiente, A.; Rodríguez-Ramos, L.; Guerrero-Ruiz, A. *Thermochim. Acta* **2001**, *379*, 195–199.
- (28) Liu, W.; Zhu, Y. F.; Lian, J. S.; Jiang, Q. *J. Phys. Chem. C* **2007**, *111*, 1005–1009.
- (29) Panagiotopoulou, P.; Kondarides, D. I. *Catal. Today* **2006**, *112*, 49–52.
- (30) Greenler, R. G. *J. Chem. Phys.* **1962**, *37*, 2094–2100.
- (31) Kagel, R. O. *J. Phys. Chem.* **1967**, *71*, 844–850.
- (32) Kagel, R. O.; Greenler, R. G. *J. Chem. Phys.* **1968**, *49*, 1638–1647.
- (33) Evans, H. E.; Weinberg, W. H. *J. Chem. Phys.* **1979**, *71*, 1537–1542.
- (34) Zhang, J.; Zhong, Z.; Cao, X.; Hu, P.; Sullivan, M.; Chen, L. *ACS Catal.* **2014**, *4*, 448–456.